Movements of HIV-virions in human cervical mucus

Hacène Boukari[1,*], **Beda Brichacek**[1], **Pamela Stratton**[2], **Sheila F. Mahoney**[2], **Jeffrey D. Lifson**[3], **Leonid Margolis**[1], and **Ralph Nossal**[1]

[1]Program in Physical Biology, Eunice Kennedy Shriver National Institute of Child Health and Human Development, Bethesda, MD 20892

[2]Program in Reproductive and Adult Endocrinology; Eunice Kennedy Shriver National Institute of Child Health and Human Development, Bethesda, MD 20892

[3]SAIC Frederick, National Cancer Institute, Frederick, MD 21702

Abstract

Time-resolved confocal microscopy and fluorescence correlation spectroscopy were used to examine the movements of fluorescently-labeled HIV virions (~100 nm) added to samples of human cervical mucus. Particle-tracking analysis indicates that the motion of most virions is decreased 200-fold compared to that in aqueous solution and is not driven by typical diffusion. Rather, the time-dependence of their ensemble-averaged mean-square displacements is proportional to $\tau^\alpha + v^2\tau^2$, describing a combination of anomalous diffusion ($\alpha \sim 0.3$) and flow-like behavior, τ being the lag time. We attribute the flow-like behavior to slowly-relaxing mucus matrix that follows mechanical perturbations such as stretching and twisting of the sample. Further analysis of the tracks and displacements of individual virions indicates differences in the local movements among the virions, including constrained motion and infrequent jumps, perhaps due to abrupt changes in matrix structure. Changes in the microenvironments due to slow structural changes may facilitate movement of the virions, allowing them to reach the epithelial layer.

I. Introduction

A distinct mucus layer coats the luminal surfaces of many epithelial tissues. Mucus is a biogel predominantly made up of water (~95%), containing gel-forming mucins (~3%) and varying amounts of degradative enzymes, antibodies, and other macromolecules[1-4]. Depending on its location, it also may contain cells (e.g., squamous cells, bacteria), cell debris, viruses, DNA, and lipids. Mucus has multiple important functions including lubrication, hydration and, in particular, protection of tissue surfaces. Several studies have indicated the role of mucus as a barrier against pathogens, although detailed mechanisms are still unclear[5-7]. In the case of the female reproductive tract, cervical mucus, in particular, may provide defense against viruses. Better understanding of the properties of cervical mucus might lead to the development of new protective measures, especially against HIV transmission[8,9].

In this study we focus on the movement of HIV virions through human cervical mucus, the latter, along with other vaginal secretions, forming a biological layer that the virus must penetrate in the course of heterosexual transmission[10]. We used unprocessed, crude cervical mucus provided by healthy donors, and measured the transport of the HIV-virions in each sample individually. Although the mucus changes over the menstrual cycle, becoming thinner and more watery at ovulation and thicker and less penetrable later in the cycle[11,12], we aimed

*To whom correspondence should be sent. Currently appointed in the Department of Anatomy and Structural Biology, Albert Einstein College of Medicine, Bronx, NY, USA.

to reproduce as much as possible the conditions -particularly the structural microenvironments - which the virions would encounter while moving through each individual sample.

The optical techniques of fluorescence correlation spectroscopy[13-15] (FCS) and time-resolved fluorescence confocal microscopy (TRFCM)[16,17] were used to probe the dynamics of fluorescently-labeled HIV-virions and other fluorescent nanoparticles (i.e Alexa 488, phycoerythrin proteins, polystyrene beads) within human cervical mucus samples. FCS, based on fluctuations in the number of fluorescent nanoparticles in an irradiated volume, is useful for obtaining information on the diffusion and binding of small, fast moving nanoparticles in a small volume (~femtoliter). In contrast, TRFCM provides insights into the spatial distribution and the movement of relatively large and/or slow nanoparticles. Furthermore, three-dimensional confocal images can be generated to capture the spatial distribution of the nanoparticles (polystyrene latex beads and HIV-virions), yielding information on the microstructure of the host mucus.

In the work reported upon in this paper, HIV virions were added, in vitro, to the mucus samples, the movements of the virions were tracked individually, and the mean-square displacement (MSD) of each virion was calculated as a function of time. The ensemble-averaged MSD of all virions detected within a given sample then was computed and its time-dependence compared with those of the individual virions. It is apparent that any particular mucus sample is structurally quite heterogeneous, but that, at least for the conditions studied here, the virions are either trapped or move very slowly, in the latter instance showing a combination of anomalous diffusion and flow-like motion.

II. Samples and Methods

II.1 Samples

Mucus Samples—Specimens of cervical mucus were collected from non-HIV infected, generally healthy female donors by aspiration, using an endometrial suction curette (Unimar Pipelle, CooperSurgical, Shelton, CT). Study participants were premenopausal and did not show evidence of genital tract infection. Information on patient age, cycle day, and use of hormones and medication was recorded for all subjects. Samples were discarded if they were bloody. The samples were carried on ice, stored at 4°C, and were typically studied within 48 hours from the collection time.

We qualitatively assessed the elasticity of the samples by gentle stretch and measured their pH. In our study we used only samples that had been collected in mid menstrual cycle. All showed similar elastic properties, springing back to their original shape, and their pH was close to neutral, in accord with previously published data[18]. Without further manipulation, mucus specimens were deposited onto a sample holder (see below) and subject to a change of temperature from physiological to room temperature (ca. 20° C). Some samples were optically turbid due to the presence of cells (e.g., squamous cells) and other large scatterers, but we were able to find relatively clear spots for imaging. We analyzed four specimens in detail, which was sufficient to establish methodology and demonstrate certain characteristic behaviors. At least five separate microscope fields were processed for each sample, on average there being ten virions per field. For analysis, close to 50 different virus particles were tracked.

Labeled HIV Virions—HIV-1 virions (viral strains MN) were inactivated and internally labeled with the NEM analog Alexa Fluor 488 C5 maleimide (Fluorescent Probes, Invitrogen, Eugene, OR) to alkylate cysteines of zinc fingers of the HIV-1 nucleocapsid protein[19]. Since disulfide-bonded cysteines of the envelope glycoproteins were unaffected, the functional properties of the viral envelope were preserved. The purified Alexa Fluor 488 labeled virions were stored in PBS buffer at −80°C. For use, the virions were thawed, gently mixed, and

centrifuged at 14000 rpm (~16000 g) in an Eppendorf MicroCentrifuge 5415C for 3 minutes to remove any aggregates formed during storage.

Fluorescent nanoprobes—The interactions with cervical mucus of several fluorescent probes, including Alexa Fluor 488 molecules (MW≈885 Da) and phycoerythrin proteins (MW≈240 kDa, diameter ≈11 nm), both obtained from Invitrogen, were investigated by confocal microscopy and fluorescent correlation spectroscopy. Structural features of mucus were discerned with the addition of green fluorescently-labeled polystyrene beads[20] (diameter: 28, 51 nm) purchased from Duke Scientific Corp. (now, Thermo Fisher Scientific, Waltham, MA).

Preparation of samples for microscopy—The sample holders consisted of two glass standard coverslips (size: A) separated by a ~200 μm thick rubber spacer containing a 5-mm diameter hole. In order to minimize interactions with virus, the coverslips were treated with Sigmacote (Sigma-Aldrich, Saint Louis, MO, USA), which reacted with silanol groups on the glass surfaces, producing a neutral, hydrophobic thin film. To clean residues from the reaction, the coverslips were washed several times with methanol and later soaked in water for at least 30 minutes.

Using a pipette, a small sample (~20 μl) of the mucus was placed in the sample holder, after which a 1-2 μl aliquot of the concentrated solution of the HIV-virions was added. The virions were introduced into the mucus by gently and slowly inserting the tip of the pipette into the sample, to reduce distortions of mucus structure that could arise using techniques involving stirring.

II.2 Experimental Techniques and Data Analysis

Fluorescence Correlation Spectroscopy (FCS)—The basic principles of FCS have been described previously[13-15]. A focused laser beam was used to excite the fluorescence of target nanoparticles, and the signal emitted from a small volume (~femtoliter) was measured as a function of time. Due to movement of the nanoparticles in and out of this small volume or changes in the photodynamics of the nanoparticles, the emitted fluorescence signal fluctuated. Analysis of the temporal intensity-intensity correlation function yielded the apparent diffusion time, which characterized the movement of the nanoparticles across the detected small volume, and, more interestingly, was related to the overall size and shape of the nanoparticles[15,21].

FCS measurements were made with a portable unit marketed by Hamamatsu (Bridgewater, NJ, USA.) This unit (model C9413) was equipped with a 473 nm LD-pumped solid-state laser, a high sensitivity photomultiplier tube with low afterpulsing, a 25 μm diameter pinhole for confocal detection, a water-immersion objective (Olympus UApo 40X W/340; NA=1.15), and built-in numerical code for correlating the time-sequence of the photocounts. In most measurements, the 1 mW input laser beam was attenuated to 3 μW and the cut-off wavelength of the high-band emission filter was set to 495 nm. Fitting of the measured correlation functions and calculation of photocounting histograms were performed using the software package developed by Hamamatsu and supplied with the instrument.

Time-Resolved Fluorescence Confocal Microscopy (TRFCM): Virus particles and polystyrene latex spheres were examined with a custom-built confocal microscope system consisting of an IX70 inverted microscope (Olympus, Center Valley, PA, USA), a confocal spinning disk analyzer (Perkin-Elmer, Fremont, CA) attached to a cooled 512X512 CCD camera (Model C9100, Hamamatsu, Bridgewater, NJ, USA), an air-cooled ion-argon laser (Melles-Griot, Carlsbad, CA, USA) with two basic excitation lines (488 nm and 568 nm), a

piezo-electric driven device (Physik Instrumente, Karlsruhe/Palmbach, Germany) for z-positioning of the objective, and a 2D XY-Proscan stage (Prior, Rockland, MA, USA).

The system was set on a low-vibration insulation table (Newport, Irvine, CA, USA). Most of the images were collected with a 60X, NA=1.2 water Olympus objective. IPLab™ software (BD Biosciences, Rockville, MD, USA) was used to control various devices, and to acquire and analyze images.

Image analysis and Particle Tracking—Fluorescent confocal images were taken with 488-nm excitation. In the present report, we describe images taken from mucus samples in which either fluorescent polystyrene beads (28-nm) or fluorescent HIV-virions were embedded. Here, z-stacks of images were collected at 1 μm steps over 20 to 40 μm heights and further processed to create 3-dimensional images of the samples. By calculating the Fourier transform of the images, we were able to assess possible alignment and orientation of the fluorescent features in the images.

To analyze the movements of the HIV virions within the mucus, we collected a time-series of 100 images over a 15 second period (100 ms exposure time and ~50 ms delay time between images.) The observed focal plane was always kept 50 μm away from the surface of the bottom coverslip to avoid boundary effects. The exposure time of each image was set typically between 50 and 100 ms, depending on the brightness of the fluorescent probes. By switching to continuous bright-white transmission illumination, we checked that the imaged field was free of large features such as cells or unknown debris. In the 512X512 digital images the fluorescent virions appeared as bright spots, the average number of which per image was about 10. Using a custom-made algorithm encoded with MatLab software, we simultaneously tracked these virions and determined changes of the spatial coordinates $(X(t), Y(t))$ of the center of mass (centroid) of the intensity profile of each individual virion with time. Based on the photon-counting histogram, we considered only spikes with average fluorescence intensities at least twice that of the background.

To quantify the movement of the virions and following the approach described by Qian et al. [16], we calculated the mean-square displacement (MSD) of each individual virus particle: MSD $(\tau)=<[X(t+\tau)-X(t)]^2> + <[Y(t+\tau)-Y(t)]^2>$, t and τ denoting the time and the "lag time," respectively. Further, we computed the ensemble-averaged[16,17] MSD's of all virions (41 virions in total), regardless of their individual dynamical behavior.

III. Results

III.1 Polystyrene beads bind to mucus

In Figure 1a, an image of fluorescent 28-nm polystyrene beads decorating a mucus sample clearly demonstrated the existence of filamentous bundles. By performing fast Fourier transformation of the images, the angular orientation of the filaments was highlighted (see Fig. 1b), confirming the alignment of multiple bundles. Similar ribbon-like, fibrillar structures were previously observed at the local level in unstretched mucus samples which had been fixed for electron microscopy[22]. Although it is possible that the beads tend to induce macroscopic bundling[20], the qualitative appearance of the bundles is unaffected by the size of the beads (data not shown); furthermore, even in the absence of beads, HIV virions in mucus seem to orient with respect to each other along given directions, suggesting an intrinsic structural alignment of the mucus (Fig.1c, see below).

III.2 Small nanoprobes diffuse in mucus

From FCS measurements, the Alexa488 fluorophores and phycoerythrin proteins appeared to be mobile within the samples of cervical mucus. When compared with their respective diffusion in water, Alexa488 fluorophores moved unhindered through the matrix whereas phycoerythrin (~10.2 nm) was slowed down by approximately a factor of three.

III.3 HIV-virions align along the filamentous bundles of mucus

Using FCS measurements on samples of HIV-virions diluted in water, we estimated the size of the HIV-virions, based on the Stokes-Einstein relation, to be 100-120 nm, consistent with published values estimated by cryoelectron microscopy[23,24]. When mixed into samples of cervical mucus and illuminated at 488 nm, the virions appeared in confocal images as bright spots. Over the experimental period (1-2 hours) the virions showed little dispersion in the mucus and tended, instead, to localize in some areas of the mucus, unlike their behavior in water where the virions dispersed readily. A z-stack of confocal images indicated that the virions were distributed in 3-dimensions. When we projected the 3-D stack of these images into one single 2-D image, Fourier transformation indicated alignment of the virions (Fig.1c), probably reflecting their interaction with filamentous bundles observed in the host mucus structure (Fig.1a and Fig.1b.)

III.4 HIV-virions exhibit anomalous diffusion and flow-like motion

Figures 2, 3 and 4 illustrate the two dimensional movement of three different virions in the same field of view. They exhibited different, dynamic behaviors: The motion of the virion in Fig. 2a appeared constrained, with only local motion within the site, as was inferred from the lack or weak temporal dependence of the fluctuations of the coordinates (Fig. 2b). In contrast, the virion in Fig. 3a showed an overall unidirectional drift in addition to local fluctuations (also seen in Fig. 3b). The virion in Figure 4a underwent a combination of local motion and drift punctuated by a sudden jump from one site to another (see also Figure 4b).

The insets in Figs. 2a, 3a, and 4a show the time-dependence of the corresponding MSDs. As expected, the MSD of the constrained virion (Fig. 2a) had a very weak dependence on the lag time, whereas the MSD of the virions in Figs. 3a and 4a showed a positive curvature, indicating possible combination of mechanisms of motion such as anomalous diffusion and flow-like movement. The latter is consistent with local orientation of mucus microstructure in response to stress[22], as inferred from *in vitro* studies of sperm moving in flat tubes[25] and as suggested in sperm penetration of the cervix[26]. Estimates of pore dimensions in cervical mucus range, in one report[20], from *ca.* 20 to *ca.* 200 nm and, in another[22], from *ca.* 10^2 to *ca.* 10^3 nm.

In Fig.5, we plotted the ensemble-averaged MSD of the virions of 5 different fields as a function of time (total virions = 41). We surmised that the movement of the virions is governed by two mechanisms: anomalous diffusion proportional to a power law ($\sim\tau^\alpha$) and flow-like behavior proportional to τ^α. If the two mechanisms were not coupled, the MSD of the virions could be described by the following expression:

$$<MSD>=\Gamma\tau^{\alpha}+v^2\tau^2, \tag{1}$$

where $<..>$ denotes the ensemble average, α describes the anomalous diffusion, Γ is a constant, and v characterizes the apparent velocity of the flow. For $\alpha=1$, this expression describes a pure diffusion-flow dynamics (see discussion by Qian et al.[16]). When we fit the data with the above expression, we determined the following values for the parameters: $\alpha= 0.3$, $\Gamma = 0.023$ $\mu m^2/s^{0.3}$, and v = 0.03 $\mu m/s$, demonstrating the underlying slow movements of the virions.

Compared with the diffusion in water, the virions were slowed down by approximately 200 times (estimated at $\tau = 1$ sec).

IV. Discussion

Heterosexual transmission is a major factor in the world-wide HIV/AIDS epidemic and, among adults, women account for more than half of all new cases[27-29]. Multiple biological barriers exist that inhibit virus infection of a potential host[6,30], including the mucus that covers the female genital tract, forming a protective layer against HIV invasion. The mechanisms of movement of the HIV virions through human cervical mucus are the focus of the present report. Our study confirmed that cervical mucus is very heterogeneous, as others have observed[5,20, 31-33]. The polystyrene beads bounded tightly to the mucus and demonstrated its filamentous structure. While small fluorophores appeared to move unhindered through the mucus, larger molecules such as moderately-sized proteins were slowed down several fold compared to their motion in water. The mucus retarded the movement of fluorescent HIV, about 200 fold, as compared to that of the virions in aqueous solution. Although not completely immobile, at least over the observation period (~15 s), the virions appeared to be trapped by the mucus, similar to findings by Maher et al[5]. We analyzed the trajectories of multiple virions, which were derived from a time-series of images collected on several mucus samples in which fluorescent virions were embedded. Further, following the approach described by Qian et al.[16] we calculated the time-dependence of the MSD of each individual virion as well as the ensemble-averaged (mean value) MSD of all virions (41 in total). Detailed analysis showed a combination of two mechanisms of motion: anomalous-diffusion and flow-like motion.

Fluorescence recovery after photobleaching (FRAP) and time-resolved microscopy also have been used to study the movements of various biologically-relevant macromolecules (e.g., immunoglobulins) and different viruses through samples of cervical mucus[20,31-33]. Like HIV, herpes simplex viruses (180 nm) slowed down when suspended in the mucus preparations[20]. Related investigations show that, depending on surface chemistry, the movement of 100-nm, nanoscopic polystyrene beads is retarded in the mucus 200 to 2400-fold compared to water[20,33]. However, the size of the nanoparticle accounts only partially for this slowing down, since the movements of larger polystyrene beads (200 and 500 nm) that are coated with polyethylene glycol are inhibited by but a 4 to 6 fold factor[33]. We thus infer that other properties of the virions, e.g., the charge on their surfaces, may affect their motion within mucus.

The use of ensemble averaging tended to blunt differences in viral motion which may exist because of local mucus microenvironments or structural characteristics of the virions. In Fig. 6, the plotted MSD's of individual virions all belonged to the same field of view. However, some virions showed anomalous diffusion over a wide range of time, with their MSD's proportional τ^α with ~ 0.07-0.37, and others showed a combination of anomalous diffusion and flow-like movement (MSD = $\Gamma\tau^\alpha + v^2\tau^2$). In similar studies of polystyrene beads embedded in entangled F-actin networks, Wong, et al. observed anomalous diffusion of their probes (MSD ~τ^α;$\alpha<1$) when the bead size is close to the lattice mesh size[20]. Moreover, they showed that this anomalous diffusion results from discrete, rapid movement from one microscopic site to another; without these jumps the probes would have been constrained, resulting in a MSD independent of time. Similarly, jumps may be the underlying mechanism for the observed anomalous diffusion in this study.

While the observed anomalous diffusion can be attributed to thermal fluctuations and local dynamics of the mucus, the mechanism behind the flow-like behavior is less clear. A systematic mechanical drift in the microscope setup might drag nanoparticles in a particular direction. However, this was not evident in our case when the XY-movements of different virions in the same field of view were compared. A second possible cause of the flow-like behavior could

be the drying of the mucus. Although slow evaporation of water was hard to assess, we doubt that this was the reason for virion movement since we tightly sealed the sample chambers. We think that the flow-like motion was linked to structural rearrangement and/or relaxation of the mucus following its handling. For example, following mechanical perturbations such as stretching, which might occur during loading into the sample holder, mucus may undergo slow structural relaxations. As the strained mucus relaxes, it drags the entrapped virions. These relaxations might be collective, as the mucus structure often appears to be a network of fibers[34]. It is possible that similar behavior takes place *in vivo,* as it is likely mucus is stretched during coitus.

Fourier analysis of the images indicated alignment of the virions (see Fig.1c), similar to the pattern observed with polystyrene beads decorating the filamentous bundles of mucus observed in Fig. 1a. These observations are in accord with electron-microscopy images of the bundles formed by mucin filaments[3,20,34,35].

Although our results demonstrate that HIV virions interact with mucus, the molecular mechanisms of these interactions have yet to be elucidated. Despite numerous studies, a consensus on the structure of cervical mucus (and mucus in general), be it on nanometer or millimeter length scales, is unclear. This task is complicated by the fact that mucus structure can be affected by handling and sample preparation. Moreover, natural cervical mucus contains variable amounts of mucins, water, cells, and cell debris and changes during the menstrual cycle. As described, above, in Samples and Methods, we here studied only mid-cycle mucus. To better control the properties of their samples, several investigators have focused on studies of solutions prepared with purified mucins, the major gel-forming macromolecules. Bansil and Turner[3] described mucins as multiblock copolymers with alternating polyelectrolyte domains, having both hydrophobic and hydrophilic regions, an ability to form H-bonds, and containing both positively and negatively charged moieties that can enter into electrostatic interactions. Under particular solution conditions, ordered structures were observed[36], which might be related to the bundles observed in the present study. Although one should be cautious in extrapolating the properties of solutions of pure mucins to those of the fresh natural mucus used in the current work[36,37], one can infer that mucin structures in the mucus may play a central role in attracting and trapping HIV-virions and, more generally, other pathogens. Also, the surface chemistry of nanoparticles can significantly affect their dynamics in a host medium[33,39]. Analyses of HIV-1 virions demonstrate significant variation in their surface charge[40,41], and it has been suggested that the manipulation of charge perhaps can be exploited to prevent infection[42,43]. However, in addition to such variability in the nominal charge of the virions, the effective charge may depend on properties of the host medium, such as pH and salt concentration. The methods demonstrated here can be used for systematic studies of the influence of these and other factors on virus-mucus interactions, including those linked to the menstrual cycle[35]. Such studies may have important clinical relevance, especially in the design of microbicides[44]. Mucus, together with innate anti-viral proteins, may under appropriate physiological conditions selectively inhibit the transmission of HIV-1 virions[30].

Lastly, we should like to stress that, despite the importance of various types of mucus in many physiological processes and in the maintenance of human health, relatively little is known about the physical properties of these materials. This is especially true when one takes into consideration the complications associated with real mucus. Much work yet can be done on this subject. For example, Celli et al.[36] used dynamic light scattering to study the microscopic motion of *solutions* of porcine gastric mucins (where, interestingly, a stretched exponential characterizes some of the data, albeit with a different exponent than is noted in our study — see Eq. 1, ff.); similar techniques might be used to investigate the local lattice motions of cervical mucus. Also, although beyond the scope of this study, the movements of the 'immobilized' viruses might be analyzed via a 'generalized Stokes-Einstein equation' to

provide information about the viscoelastic properties of the mucus [45]. Theories based on a Langevin equation with Levy noise[46] or a barrier-fluctuation (semi-Markov) model[47] might be developed to relate the frequency and magnitude of the observed viral 'jumps' to the relaxation of the lattice, leading to the design of experiments in which a controlled amount of uniaxial stress is applied to the mucus samples prior to making the microscopy measurements.

V. Conclusions

The displacements of HIV virions within intact cervical mucus are much slower, by two orders of magnitude, than when in aqueous solution. Analysis of the tracks of individual virions, as observed by time-resolved confocal microscopy, indicates that the virions are mostly trapped in the mucus, being constrained to small regions, and demonstrating twitching motions as if moving with the polymer lattice. This motion occasionally is punctuated by jumps to sites that are several virus lengths away, such movement perhaps being related to the mechanical relaxation of previously stressed, metastable regions of the mucus. When the ensemble-averaged mean-square displacement (MSD) of the virions is plotted as a function of time, one finds that their movement can be characterized mathematically as the sum of a term representing anomalous diffusion, proportional to a time variable having a non-integral power-law dependence ($\sim\tau^{\alpha};\alpha=0.3$), and a term denoting possible flow-like behavior ($\sim\tau^{2}$). However, the MSD's of individual virions show different values of α, perhaps linked to variation in the surface properties of the viruses and/or heterogeneities in mucus structure

Acknowledgments

V. References

[1]. Carlstedt I, Lindgren H, Sheehan JK, Ulmsten U, Wingerup L. Biochem. J 1983;211:13–22. [PubMed: 6409086]

[2]. Sheehan JK, Carlstedt I. Biochem J 1987;245(3):757–762. [PubMed: 3663189]

[3]. Bansil R, Turner BS. Current Opinions in Colloid & Interface Science 2006;11(23):164–170.

[4]. Shaw JLV, Smith CR, Diamandis EP. J. Proteome Research 2007;6(7):2859–2865. [PubMed: 17567164]

[5]. Maher D, Wu X, Schacker T, Horbul J, Southern P. PNAS 2005;102:11505.

[6]. Hladik F, Hope TJ. Current HIV/AIDS Reports 2009;6:20–28. [PubMed: 19149993]

[7]. Fox-Canale AM, Hope TJ, Martinson J, Lurain JR, Rademaker AW, Bremer JW, Landay A, Spear GT, Lurain NS. Virology 2007;369:55–68. [PubMed: 17716703]

[8]. Kasse PJ, Shattock R, Moore JP. Ann. Rev. Med 2008;59:455–471. [PubMed: 17892435]

[9]. Valenta C. Advanced Drug Delivery Reviews 2005;57:692–1712.

[10]. Broliden K, Haase AT, Ahuja SK, Shearer GM, Andersson J. J. Intern. Med 2008;265:5–17. [PubMed: 19093956]

[11]. Odeblad E. Acta Obstet. Gynecol. Scand 1968;47:57–79. [PubMed: 5690885]

[12]. Wolf DP, Sokoloski J, Khan MA, Litt M. Fertil. Steril 1977;28:47–52. [PubMed: 832715]

[13]. Webb WW. Appl. Optics 2001;40:3969–3983.

[14]. Chen Y, Müller JD, Berland KM, Gratton E. Methods 1999;19:234–252. [PubMed: 10527729]

[15]. Boukari, H.; Sackett, DL. Biophysical Tools for Biologists: Vol. 1 In Vitro Techniques Methods in Cell Biology 84. Correia, JJ.; Detrich, HW., III, editors. Elsevier Academic Press Inc.; California: 2008. p. 659-678.

[16]. Qian H, Sheetz MP, Elson EL. Biophys. J 1991;60:910–921. [PubMed: 1742458]

[17]. Wong IY, Gardel ML, Reichman DR, Weeks ER, Valentine MT, Bausch AR, Weitz DA. Phys. Rev. Lett 2004;92:178101. [PubMed: 15169197]

[18]. Correa CHM, Mattos ALG, Ferrari AN. Braz. J. Med. Biol. Res 2001;34:767–770. [PubMed: 11378666]

[19]. Morcock DR, Thomas JA, Gagliardi TD, Gorelick RJ, Roser JD, Chertova EN, Bess JW Jr, Ott DE, Sattentau QJ, Frank I, Pope M, Lifson JD, Henderson LE, Crise BJ. J. Virology 2005;79:1533–1542. [PubMed: 15650179]

[20]. Olmstead SS, Padgett JL, Yudin AI, Whaley KJ, Moench TR, Cone RA. Biophys. J 2001;81:1930–1937. [PubMed: 11566767]

[21]. Boukari H, Nossal R, Sackett DL. Biochemistry 2003;42:1292–1300. [PubMed: 12564932]

[22]. Yudin AI, Hanson FW, Katz DF. Biol. Reprod 1989;40:661–671. [PubMed: 2758095]

[23]. Zhu P, Liu J, Bess J Jr, Chertova E, Lifson JD, Grisé H, Ofek GA, Taylor KA, Roux KH. Nature 2006;441:847–851. [PubMed: 16728975]

[24]. Liu J, Bartesaghi A, Borgnia MJ, Sapiro G, Subramaniam S. Nature 2008;455:109–113. [PubMed: 18668044]

[25]. Katz DF, Overstreet JW, Hanson FW. Fertil. Steril 1980;33:179–86. [PubMed: 7353696]

[26]. Mattner PE. Nature 1966;212:1479–1480.

[27]. Galvin SR, Cohen MS. Nature Reviews: Microbiology 2004;2:33–42.

[28]. Hladik F, McElrath MJ. Nature reviews: Immunology 2008;8(6):447–457.

[29]. Kozlowski PA, Neutra MR. Current Molecular Medicine 2003;3:217–228. [PubMed: 12699359]

[30]. Margolis L, Shattock R. Nat. Rev. Microbiol 2006;4:312–317. [PubMed: 16541138]

[31]. Saltzman WM, Radomsky ML, Whaley KJ, Cone RA. Biophys. J 1994;66:508–515. [PubMed: 8161703]

[32]. Shen H, Hu Y, Saltzman WM. Biophys. J 2006;91:639–644. [PubMed: 16632500]

[33]. Lai SK, O'Hanlon DE, Harrold S, Man ST, Wang YY, Cone R, Hanes J. PNAS 2007;104:1482–1487. [PubMed: 17244708]

[34]. Ceric F, Silva D, Vigil P. J. Electron Microscopy 2005;54(5):479–484.

[35]. Gipson IK, Moccia R, Spurr-Michaud S, Argüeso P, Gargiulo AR, Hill JA 3rd, Offner GD, Keutmann HT. J Clin Endocrinol Metab 2001;86(2):594–600. [PubMed: 11158014]

[36]. Celli JP, Turner BS, Afdhal NH, Ewoldt RH, Randy GH, McKinley GH, Bansil R, Erramili S. Biomacromolecules 2007;8(5):1580–1586. [PubMed: 17402780]

[37]. Raynal BDE, Hardingham TE, Thornton DJ, Sheehan JK. Biochem. J 2002;362:289–296. [PubMed: 11853536]

[38]. Habte HH, de Beer C, Lotz ZE, Tyler MG, Schoeman L, Kahn D, Mall AS. Virology J 2008;5(59):1–10. [PubMed: 18182120]

[39]. Valentine MT, Perlman ZE, Gardel ML, Shin JH, Matsudaira P, Mitchison TJ, Weitz DA. Biophys. J 2004;86:4004–4014. [PubMed: 15189896]

[40]. Clevestig P, Pramanik L, Leitner T, Ehrnst A. J. Gen. Virol 2006;87:607–612. [PubMed: 16476981]

[41]. Repits J, Sterjovski J, Badia-Martinez D, Mild M, Gray L, Churchill MJ, Purcell DFJ, Karlsson A, Albert J, Fenyo EM, Achour A, Gorry PR, Jansson M. Virology 2008;379:125–134. [PubMed: 18672260]

[42]. Beljaars L, Floris R, Berkhout B, Smit C, Meijer DKF, Molema G. Biochem. Pharmacol 2002;63:1663–1673. [PubMed: 12007569]

[43]. Ahn K-S, Ou W, Silver J. Virology 2004;330:50–61. [PubMed: 15527833]

[44]. Geonnotti AR, Katz DF. Biophys J 2006;91:2121–2130. [PubMed: 16815899]

[45]. Mason TG. Rheol. Acta 2000;39:371–378.

[46]. Jespersen S, Metzler R, Fogedby HC. Phys. Rev 1999;59:2736–2745.

[47]. Chvosta P, Reineker P. J. Phys. A (Math. Gen.) 1997;30:L307–L312.

80 μm
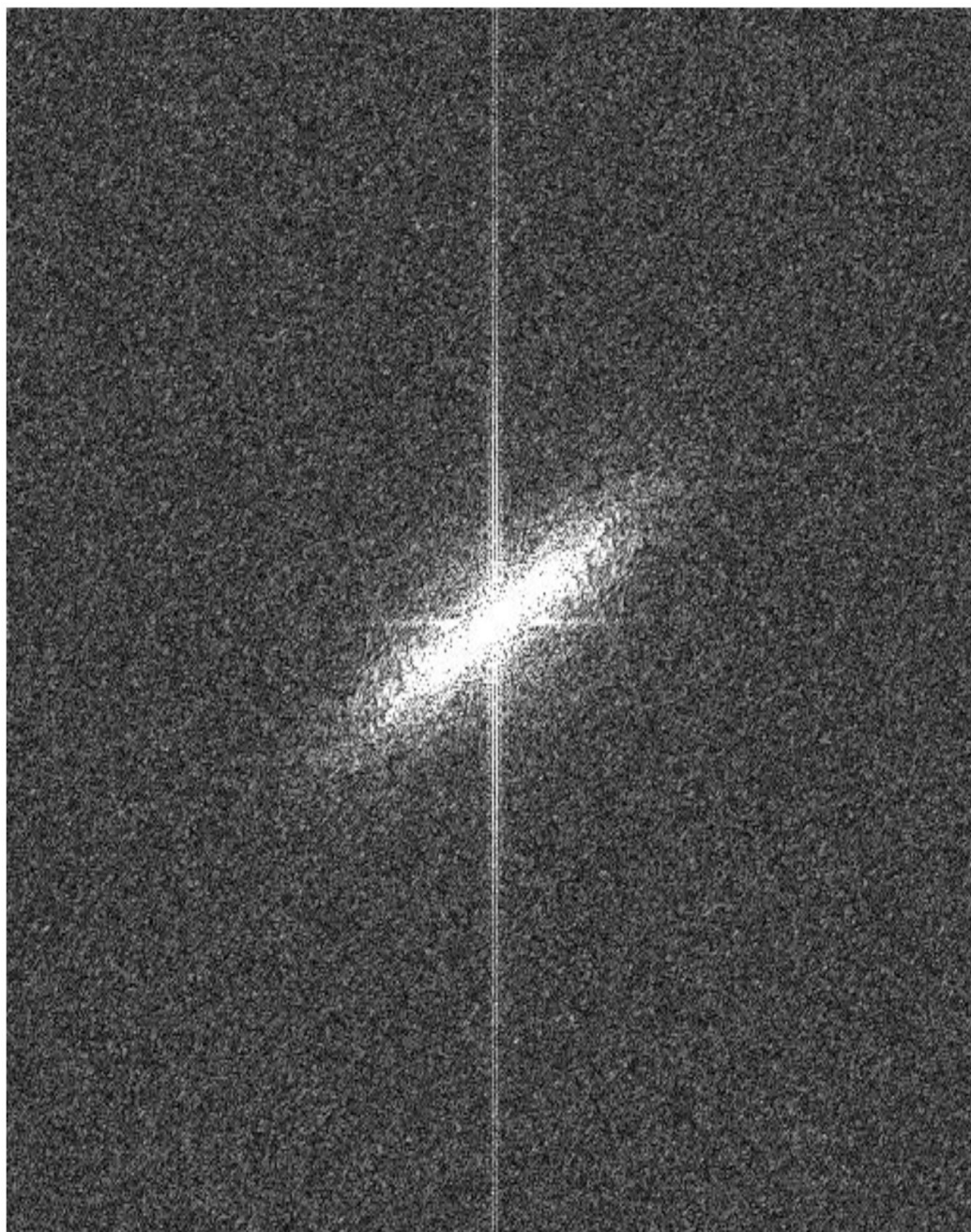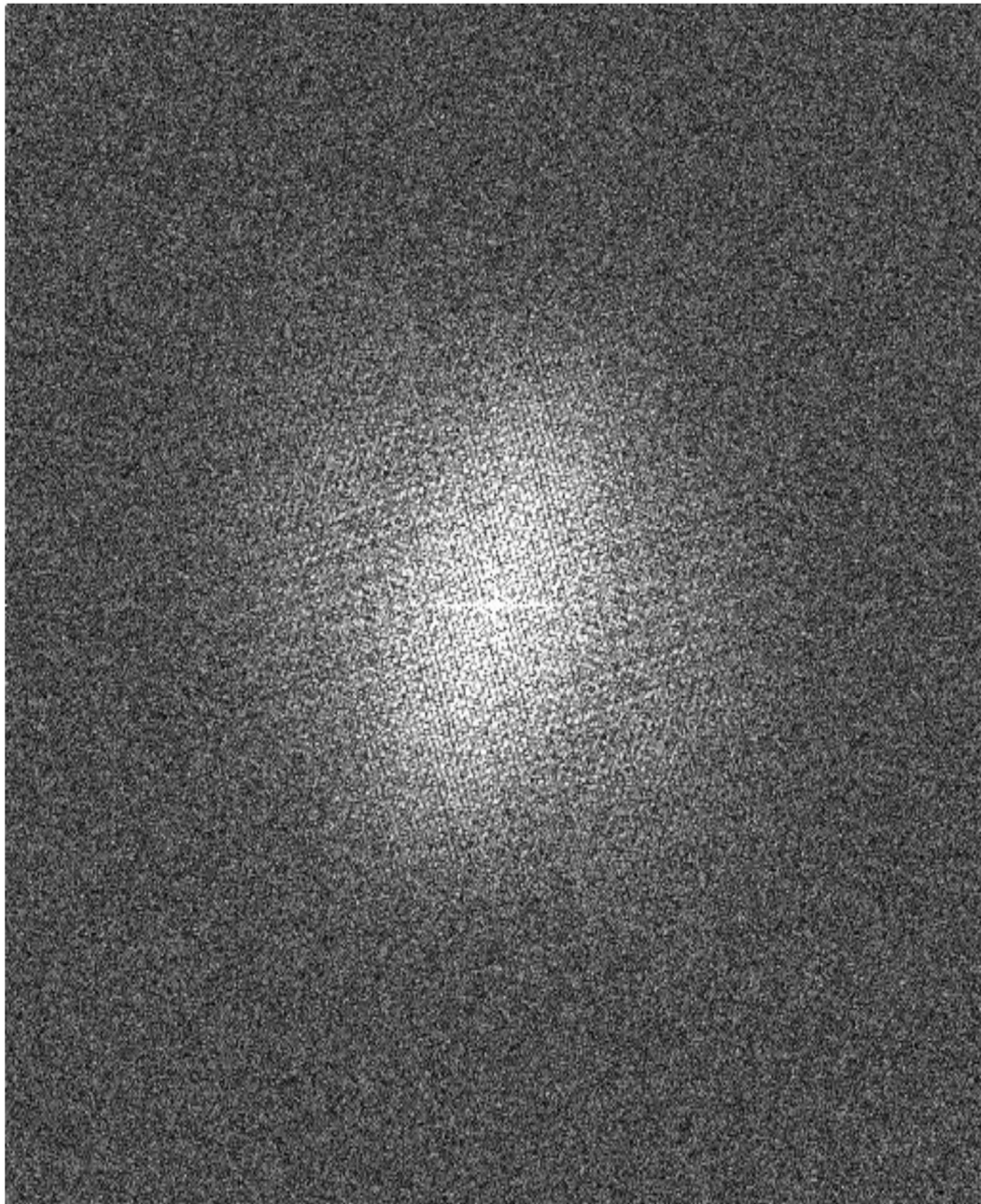
Fig.1.
A 512×512 digital image of a sample of crude human cervical mucus: (**a**) 28-nm fluorescent polystyrene beads bound to the mucus shows filamentous bundles in the mucus; (**b**) Fourier Transform of the image in Fig.1a confirms alignment of the bundles; (**c**) Fourier Transform of an image of HIV-virions embedded in the mucus indicates alignment of the virions, most likely along filamentous bundles similar to those shown in Fig.1a.
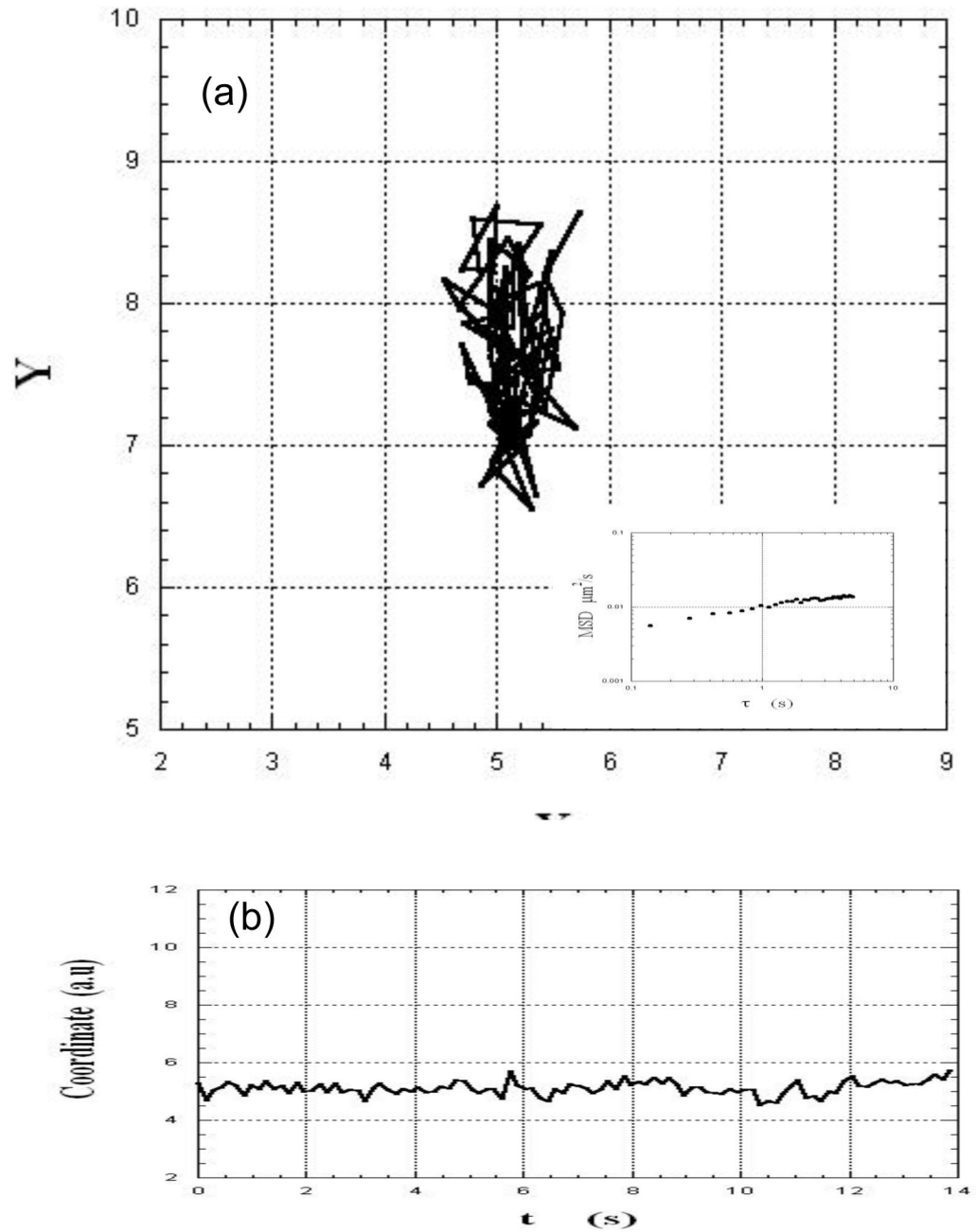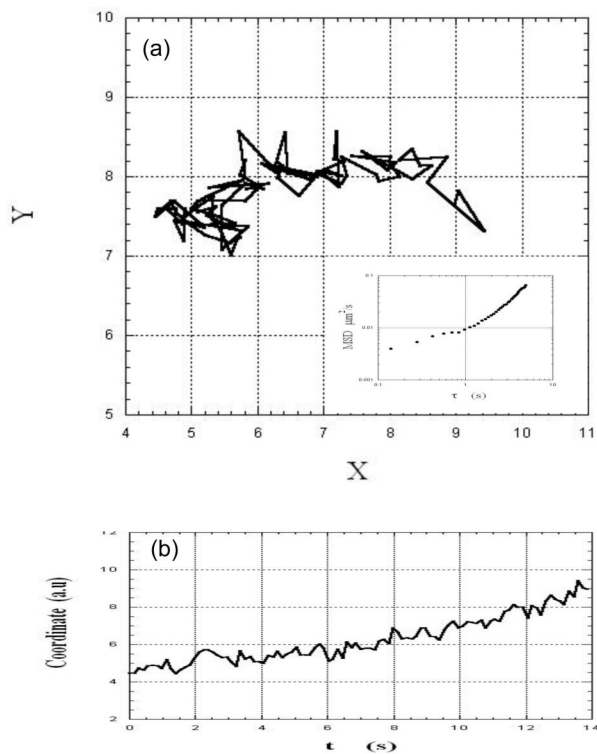
Fig.2.
(a): XY track of an HIV-virion embedded in a sample of cervical mucus shows constrained motion. The inset in (a) shows the time-dependence of the mean-square displacement of the virion (see text). (b): The time-dependence of one of the coordinates of the virion confirms the local displacement.

Fig.3.
(a): XY track of an HIV-virion embedded in a sample of cervical mucus shows local motion and drift. The inset in (a) shows the time-dependence of the mean-square displacement of the virion (see text). (b): The time-dependence of one of the coordinates confirms the systematic displacement of the virion.
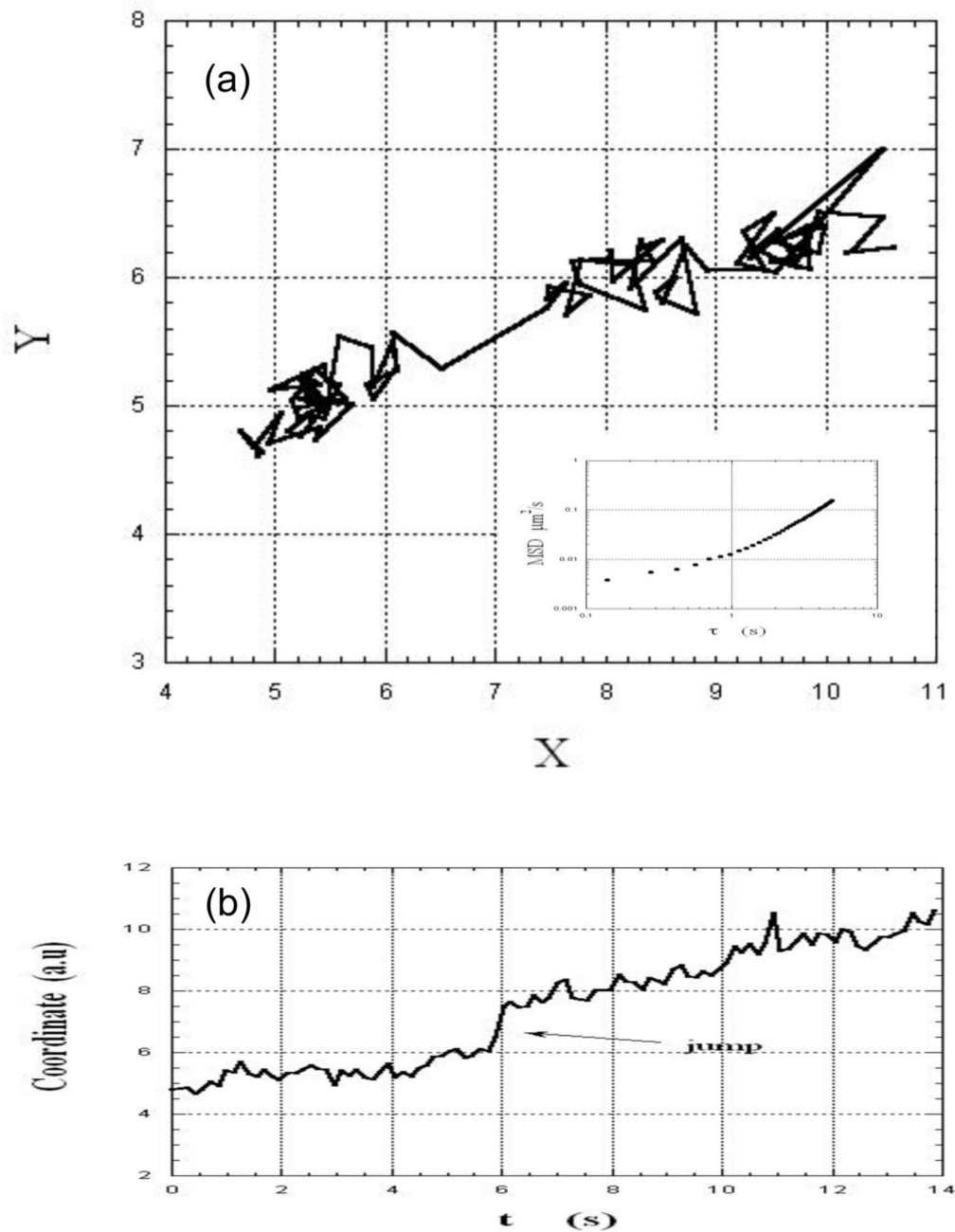
Fig.4.
(a): XY track of an HIV-virion embedded in a sample of cervical mucus shows local motion, drift, and a sudden jump. The inset in (a) shows the time-dependence of the mean-square displacement of the virion (see text). (b): The time-dependence of one of the coordinates confirms the existence of the jump as well as the systematic displacement of the virion.
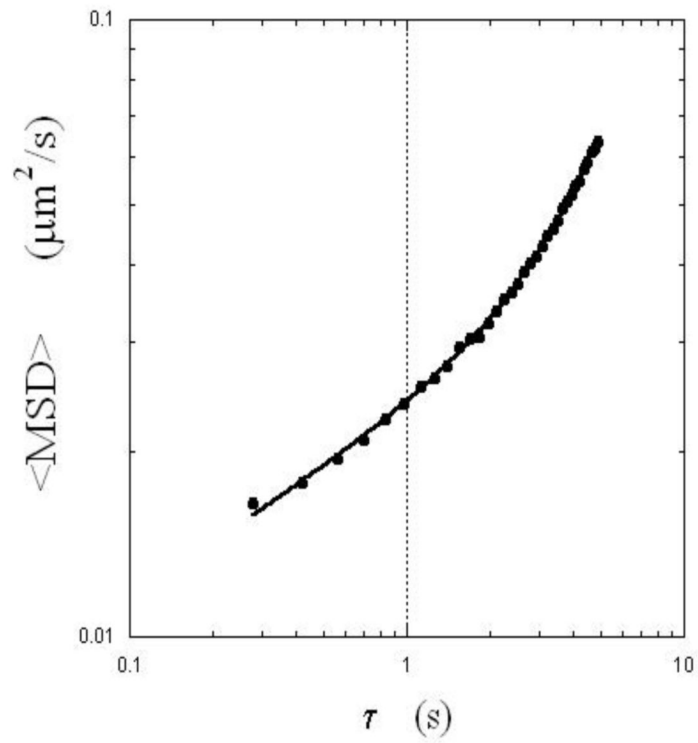
Fig.5.
Ensemble-averaged mean-square displacements of HIV-virions (41 total) are plotted as a function of lag time. The solid line is the fit with a scaled function ($A\tau^{\alpha} + v^2\tau^2$; see text), indicating anomalous diffusion and flow-like behavior.
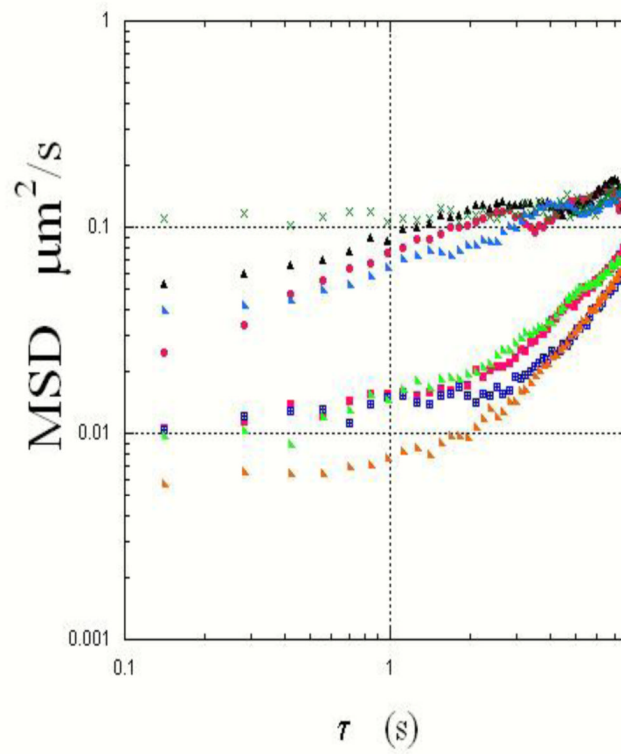
Fig.6.
Mean-square displacements of several HIV-virions observed in the same field of view are plotted as a function of time. Note the differences in the motion of the virions, perhaps reflecting differences in their structure as well as in local mucus microenvironments.